J Mater Sci (2011) 46:4509–4516
DOI 10.1007/s10853-011-5344-8

Dielectric relaxation in $Se_{80-x}Te_{20}Sn_x$ chalcogenide glasses

A. Sharma · N. Mehta · A. Kumar

Received: 27 September 2010 / Accepted: 27 January 2011 / Published online: 15 February 2011

Abstract This study reports the temperature and frequency dependence of dielectric constant (ε') and dielectric loss (ε'') in glassy $Se_{80-x}Te_{20}Sn_x$ ($x = 0, 2, 4, 6$) alloys. The measurements have been made in the frequency range (1–500 KHz) and in the temperature range 305–335 K. The results indicate that the dielectric dispersion exists in the present glassy systems in the above frequency and temperature range. The composition dependence of the dielectric constant, dielectric loss and activation energy thermally activated crystallization is also discussed.

Introduction

Chalcogenide glasses are of special interest due to their broad applications in modern electronics, optoelectronics, integrated optics, electro-photography solar cells, electrical, and optical memory devices etc., [1–10].

Selenium-based chalcogenide glasses have high transparency in the broad middle and far IR regions and have strong non-linear properties [11]. Apart from these applications, amorphous Se has been found to have tremendous potential in xeroxing applications and therefore a lot of attempts have been made to improve its properties by alloying [12] it with other elements. Alloying elements produce characteristic effects depending on the electronic structure of these elements. The Se–Te glassy alloy system based on Se is of considerable commercial, scientific and technological importance. They are widely used for various applications as optical recording media, because of their excellent laser writing sensitivity, xerography, and electrographic applications.

The glass-formation region of tin-based binary and ternary chalcogenide glasses is very narrow and corresponds to a small amount of tin in the alloy. Hence, no sufficient studies are reported in literature on tin-based chalcogenide glasses. Influence of crystallization on electrical and optical properties of Se–Te–Sn thin films is studied by Georgieva et al. [13]. Crystallization kinetics of the amorphous $Se_{80-x}Te_{20}Sn_x$ system is reported by Kaur et al. [14] using DSC technique. Kumar et al. [15] reported effect of Tin impurity and Swift heavy ion irradiation on the optical properties of the Se–Te thin films. Sharma et al. [16] reported the effect of incorporation of Sn on electrical properties of glassy $Se_{85}Te_{15}$ alloys. The band gap study on glassy films of ternary Se–Te–Sn system is reported by Saraswat et al. [17].

The study of dielectric behavior of chalcogenide glasses is expected to reveal structural information which, in effect, can be useful for the understanding of conduction mechanism as well. In addition, a study of temperature dependence of dielectric permittivity particularly in the range of frequencies where dielectric dispersion occurs can be of great importance for the understanding of the nature and origin of the losses occurring in these materials. In this study, the authors have reported the effect of Sn incorporation on the dielectric properties of glassy $Se_{80}Te_{20}$ alloy.

Material preparation

Glassy alloys of $Se_{80-x}Te_{20}Sn_x$ ($x = 0, 2, 4, 6$) system were prepared by the quenching technique. High purity

A. Sharma · N. Mehta (✉)
Department of Physics, Banaras Hindu University,
Varanasi 221 005, India
e-mail: dr_neeraj_mehta@yahoo.co.in

A. Kumar
Department of Physics, Harcourt Butler Technological Institute,
Kanpur 208 002, India

Se, Te, and Sn materials (5 N) were weighed according to their atomic percentages, and were sealed in quartz ampoules (length $\sim$5 cm and internal diameter $\sim$8 mm), with a vacuum $\sim 10^{-5}$ Torr. The sealed ampoules were kept inside a furnace where the temperature was raised to 1000 °C, at a rate of 3–4 °C/min. The ampoules were frequently rocked for 10 h at the maximum temperature to make the melt homogeneous. Quenching was done in ice water and the glassy nature was verified by X-ray diffraction. The XRD pattern of as prepared sample of glassy $Se_{80-x}Te_{20}Sn_x$ ($x = 0, 2, 4, 6$) alloys are shown in Fig. 1. Absence of any sharp peak confirms the glassy nature of the sample. X-ray diffraction patterns of $Se_{80-x}Te_{20}Sn_x$ ($x = 0, 2, 4, 6$) alloys annealed near the crystallization region (350 K) for 24 h are also shown in Fig. 1b.

The chemical composition of the samples was checked through the energy dispersive X-ray (EDX) analysis. No significant variation was found in the value of x in glassy $Se_{80-x}Te_{20}Sn_x$ ($x = 0, 2, 4, 6$) alloys.

DSC (Simdazu, Japan) was used for determination of glass transition temperature and crystallization temperature of the present samples. 5 mg of each sample was utilized to run the DSC scan at heating rate of 10 °C/min. DSC scans are shown in Fig. 2. From this figure, it is clear that well-defined endothermic and exothermic peaks are obtained in DSC thermogram showing glass transition and crystallization phenomena in the present materials.

Dielectric measurements

The glassy alloys thus prepared were ground to a very fine powder and pellets (diameter $\sim$10 mm and thickness $\sim$1 mm) were obtained by compressing the powder in a die at a load of 5 Tons. The pellets were coated with vacuum evaporated indium film to insure good electrical contact between the sample and the electrodes.

The pellets were mounted in between two steel electrodes of a metallic sample holder for dielectric measurements.

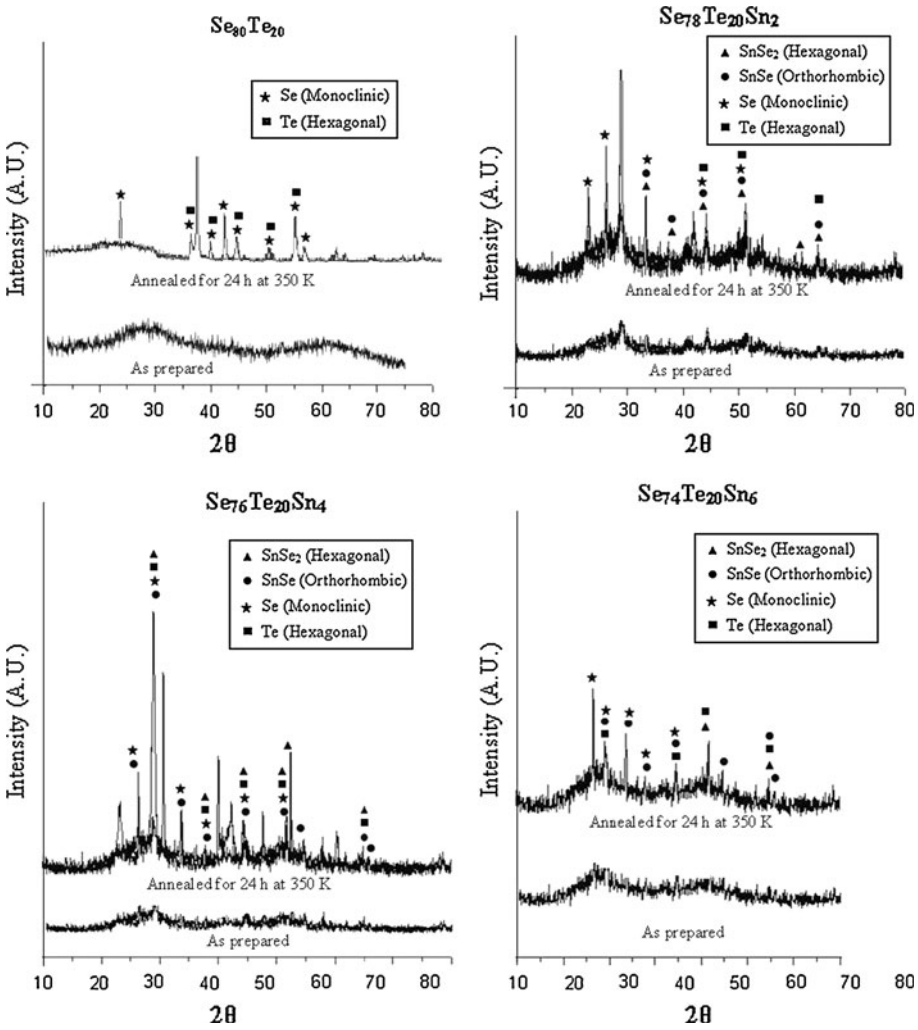

Fig. 1 XRD patterns of glassy $Se_{80-x}Te_{20}Sn_x$ alloys before annealing and after annealing for 24 h

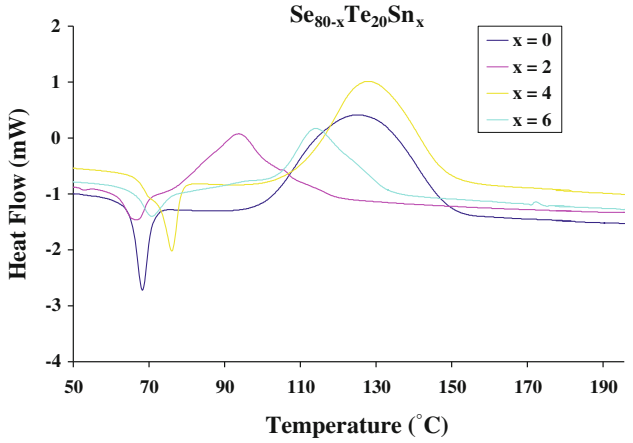

Fig. 2 DSC scans for glassy $Se_{80-x}Te_{20}Sn_x$ alloys at heating rate of 10 °C/min

The temperature measurement was facilitated by a copper-constantan thermocouple mounted very near to the sample. A vacuum of $\sim 10^{-2}$ Torr was maintained over the entire temperature range (305–335 K). The temperature dependence of ε' was studied in heating run at a heating rate of 1 K/min. Dielectric measurements were made using a digital LCR meter (Wayne Kerr Electronics, Model: 4255). The parallel capacitance and dissipation factor was measured and then ε' and ε'' was calculated. The authors preferred to experiment on the pellet rather than the bulk as macroscopic effects (gas bubbles, etc.) may appear in the bulk during preparation. It has been shown in past [18], both theoretically and experimentally, that bulk ingots and compressed pellets exhibit similar dielectric behavior in chalcogenide glasses for the suspected inhomogeneities in case of compressed pellets in these materials.

Theoretical basis

Guintini et al. [19] have proposed a model for dielectric dispersion in chalcogenide glasses. This model is based on the Elliott's idea [20] of hopping of charge carriers over a potential barrier between charged defect states (D^+ and D^-). Each pair of site (D^+ and D^-) is assumed to form a dipole which has a relaxation time depending on it's energy [21, 22], the latter can be attributed to the existence of a potential barrier over which the carriers hop [23].

According to the above model [19], ε'' at a particular frequency, in the temperature range where dielectric dispersion occurs, is given by:

$$\varepsilon''(\omega) = (\varepsilon_0 - \varepsilon_\infty)2\pi^2 N(ne^2/\varepsilon_0)^3 k\,T\tau_0^m W_m^{-4}\omega^m \quad (1)$$

where m is a power of angular frequency and is given by:

$$m = -4k\,T/W_m \quad (2)$$

Here, n is the number of electrons that hop, N is the concentration of localized sites, ε_0 and ε_∞ are the static and optical dielectric constants, respectively, W_m is the energy required to move the electron from a site to infinity.

Results

It has been reported [19–24] that, in chalcogenide glasses, the temperature dependence of ε' and ε'' is appreciable only in certain temperature range. At lower temperatures, ε' is almost constant and ε'' is negligibly small. After a certain temperature, ε' and ε'' are increased appreciably with temperature. Therefore, the present measurements have been made only in the high temperature region where dielectric dispersion is quite appreciable. The temperature dependence of ε' and ε'' are studied at various frequencies (1–500 KHz) for all the glassy alloys studied here. The temperature range of measurements is from 305 to 335 K.

Temperature dependence of dielectric constant (ε') and dielectric loss (ε'')

Figures 3 and 4 show the results of the dielectric constant and dielectric loss measurements for glassy $Se_{80-x}Te_{20}Sn_x$ ($x = 0, 2, 4, 6$) alloys. These figures indicate that the temperature dependence of ε' and ε'' is appreciable only in the certain temperature range. At lower temperatures, ε' and ε'' are found almost constant. Only after a certain temperature, ε' and ε'' are increased appreciably with temperature. In this glassy sample, dielectric constant increases with the increase in temperature, the increase being different at different frequencies. Thus, the temperature dependence of ε' and ε'' in the present chalcogenide glass is same as reported by various workers in other chalcogenide glasses [19–24].

Frequency dependence of dielectric constant (ε') and dielectric loss (ε'')

Figure 5 shows the frequency dependence of dielectric constant ε' at different temperatures for glassy $Se_{80-x}Te_{20}Sn_x$ ($x = 0, 2, 4, 6$) alloys. It is clear from the figure that ε' decreases with increasing frequency and increases with increasing temperature.

The increase of ε' with temperature can be attributed to the fact that the orientational polarization is connected with the thermal motion of molecules, so dipoles cannot orient themselves at low temperatures. When the temperature is increased the orientation of dipoles is facilitated that

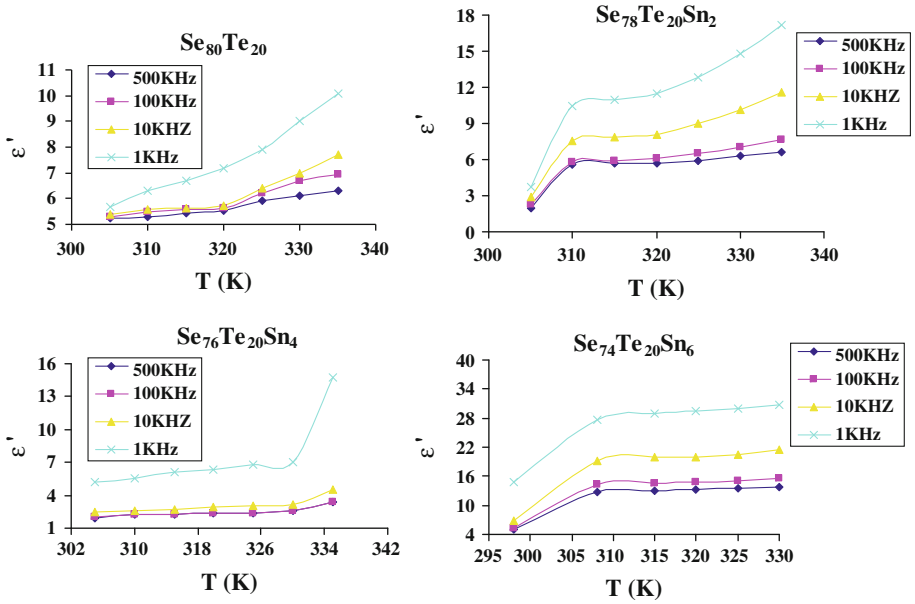

Fig. 3 Temperature dependence of dielectric constant (ε') for glassy $Se_{80-x}Te_{20}Sn_x$ alloys

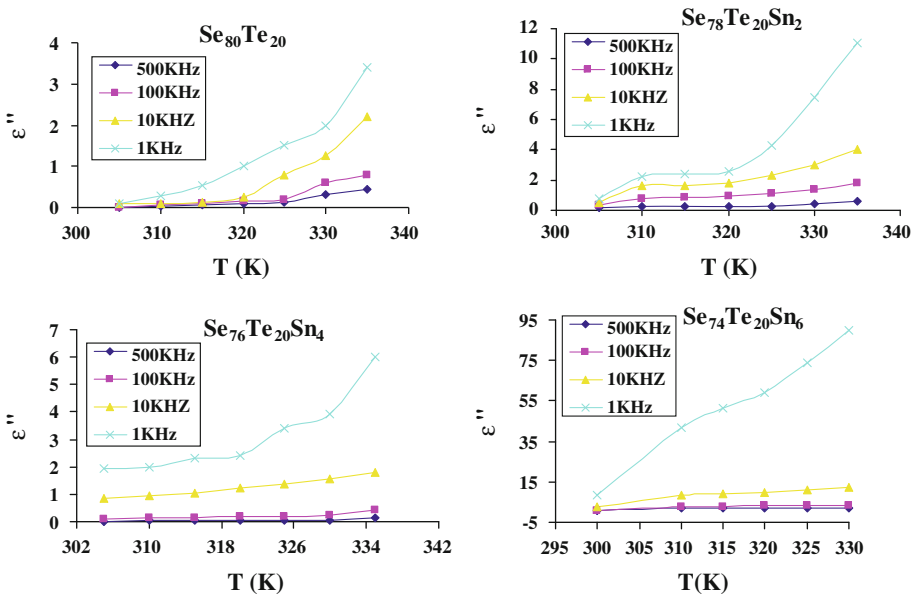

Fig. 4 Temperature dependence of dielectric loss (ε'') for glassy $Se_{80-x}Te_{20}Sn_x$ alloys

increases the value of orientational polarization. This causes the increase in ε' with increasing temperature.

The frequency dependence of dielectric loss ε'' is shown in Fig. 6 at different temperatures for glassy $Se_{80-x}Te_{20}Sn_x$ ($x = 0, 2, 4, 6$) alloys. From this figure, it is clear that ε'' is also found to decrease with increasing frequency and increase with increasing temperature according to the Eq. 2.

Composition dependence of dielectric constant (ε') and dielectric loss (ε'')

The values of dielectric constant ε' and dielectric loss ε'' at a particular frequency and temperature are given in Table 1 for glassy $Se_{80-x}Te_{20}Sn_x$ alloys. Figures 7 and 8 show the composition dependence of both parameters at same frequency and temperature. From these figures, it is clear that a reversal in the trend is observed at 4 at %.

AC mechanism in glassy $Se_{80-x}Te_{20}Sn_x$ alloys

It has been reported in many chalcogenide glasses that ac conductivity varies with frequency according to following relation [20]:

$$\sigma_{ac} \propto \omega^s, \text{ with } \quad s \leq 1 \tag{3}$$

The frequency dependence of ac conductivity for glassy $Se_{78}Te_{20}Sn_2$ alloy at different temperatures is shown in

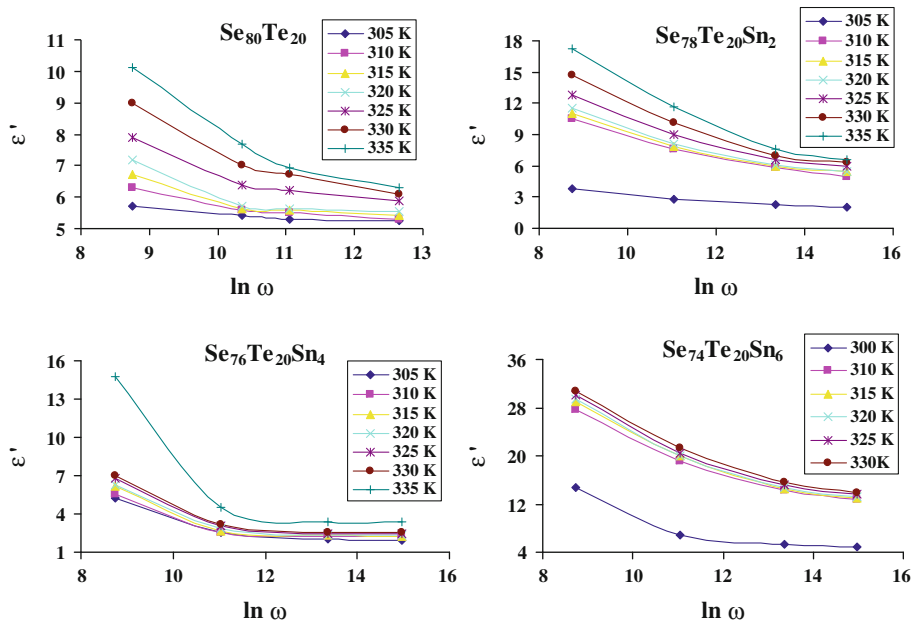

Fig. 5 Frequency dependence of dielectric constant (ε') for glassy $Se_{80-x}Te_{20}Sn_x$ alloys

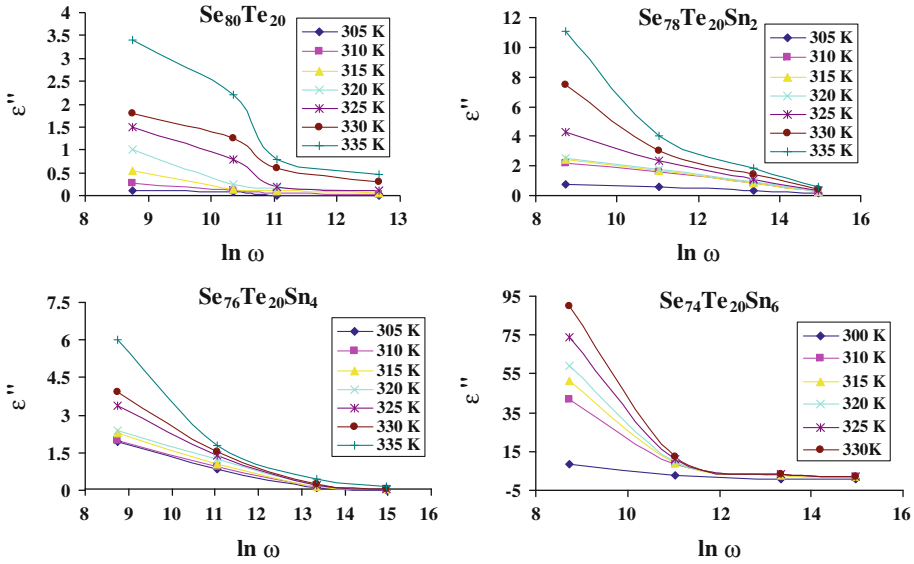

Fig. 6 Frequency dependence of dielectric loss (ε'') for glassy $Se_{80-x}Te_{20}Sn_x$ alloys

Table 1 Values of dielectric constant ε' and dielectric loss ε'' for glassy $Se_{80-x}Te_{20}Sn_x$ alloys

x	ε'	ε''
0	6.1	0.3
2	6.3	0.4
4	2.54	0.07
6	13.8	2.1

Fig. 9. From these plots, it is clear that $\sigma_{ac} \propto \omega^{s}$, where s is the frequency exponent and A is a constant. The temperature dependence of s is shown in Fig. 10. The figure clearly indicates that the values of s decrease with increasing

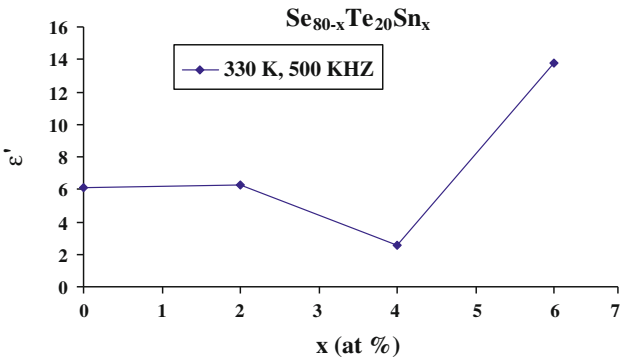

Fig. 7 Composition dependence of dielectric constant (ε') for glassy $Se_{80-x}Te_{20}Sn_x$ alloys

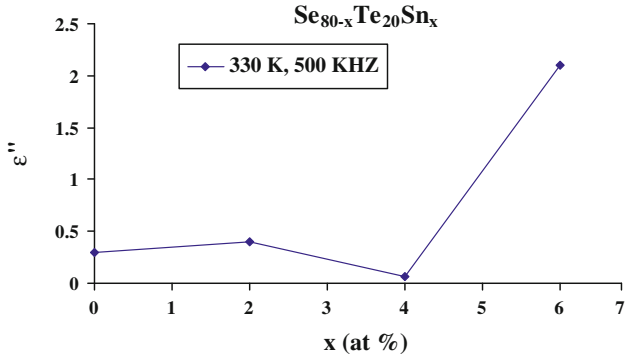

Fig. 8 Composition dependence of dielectric loss (ε'') for glassy $Se_{80-x}Te_{20}Sn_x$ alloys

temperature. Similar results were observed for other glasses. Elliott [20] suggested that such behavior of amorphous semiconductors can be explained in terms of the correlated barrier-hopping. According to this mechanism, the conduction occurs via a bipolaron hopping process wherein two electrons simultaneously hop over the potential barrier between two charged defect states (D^+ and D^-) and the barrier height is correlated with the intersite separation via a Coulombic interaction.

The temperature dependence (above the room temperature and with in the glass transition region) of ac conductivity in glassy $Se_{80-x}Te_{20}Sn_x$ ($x = 0, 2, 4, 6$) alloys is studied at different audio frequencies using the Arrheniun temperature dependence of σ_{ac}:

$$\sigma_{ac} = (\sigma_0)_{ac} \exp\left[\frac{-\Delta E_{ac}}{kT}\right] \tag{4}$$

Here ΔE_{ac} is called the activation energy for thermally activated ac conduction and $(\sigma_0)_{ac}$ is called the pre-exponential factor. The activation energy ΔE_{ac} and pre-exponential factor $(\sigma_0)_{ac}$ are determined from Eq. 4 at different frequencies for each glassy alloy. The composition

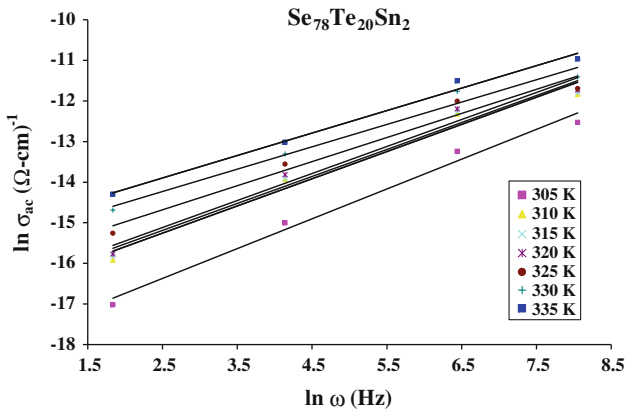

Fig. 9 Plots of ln σ_{ac} versus ln ω for glassy $Se_{78}Te_{20}Sn_2$ alloy

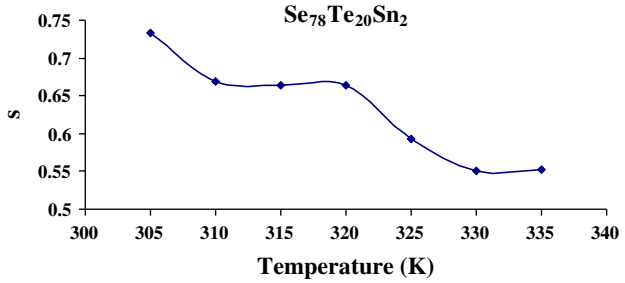

Fig. 10 Temperature dependence of exponent s

dependence of ΔE_{ac} and $(\sigma_0)_{ac}$ at a particular frequency are shown in Figs. 11 and 12. From these figures, it is clear that composition dependence of ΔE_{ac} and $(\sigma_0)_{ac}$ also have a local maxima at $x = 4$ at %. Similar results were obtained at other audio frequencies.

Discussion

The average coordination numbers $\bar{Z}$ of the studied glasses were evaluated using the standard procedure described by Tanaka [25], using coordination numbers (CN) of 4, 2, and 2 for Sn, Se, and Te, respectively. Thus, for the glassy system $Se_aTe_bSn_c$ ($a + b + c = 1$), the values of $\bar{Z}$could be given by the following relation:

$$\bar{Z} = \frac{(aZ_{Se} + bZ_{Te} + cZ_{Sn})}{(a+b+c)} \tag{5}$$

The mean coordination number$\bar{Z}$in the present glasses in this study is from 2.0 to 2.1 because Sn is four-fold coordinated and Se is two-fold coordinated. As the authors studied the smaller Sn concentrations of Se–Te–Sn glasses with $\bar{Z} < 2.4$, these glasses would be mainly of 'floppy' character [26]. Such conjecture about a glass structure implies change in medium range structural order when compared with large coordination number compositions.

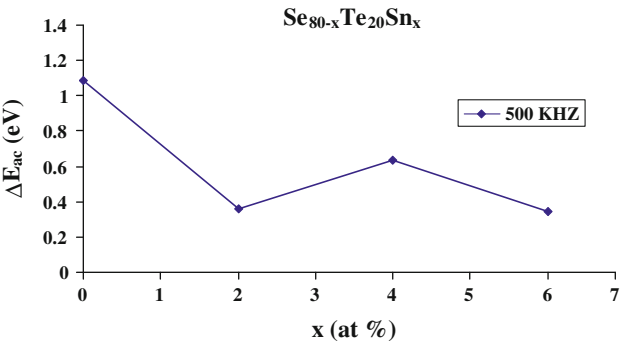

Fig. 11 Composition dependence of ΔE_{ac} for glassy $Se_{80-x}Te_{20}Sn_x$ alloys at different frequencies

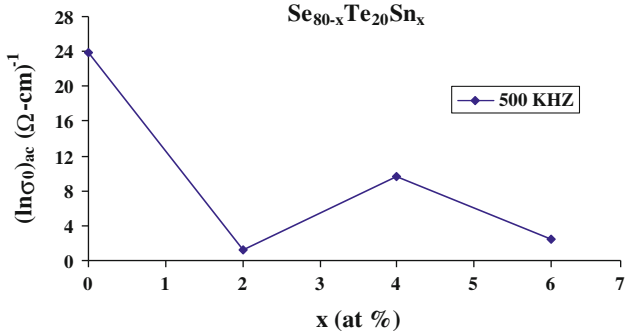

Fig. 12 Composition dependence of $(\ln\sigma_0)_{ac}$ for glassy $Se_{80-x}Te_{20}Sn_x$ alloys at different frequencies

Philips used the change in the dependence of the viscosity activation entropy versus $\bar{Z}$ to discuss the structure of chalcogenide glasses and pointed out sub regions. These sub-regions are between the coordination numbers 2–2.06, between 2.08–2.18 and 2.20–2.38. They were attributed to the formation of sub-structures with one, two and three dimensional structures [27, 28]. There are three threshold compositions, corresponding to changes in the viscosity, which are at $\bar{Z} \sim 2.07$, ~ 2.19, and at 2.40. The first corresponds to a change from one- to two-dimensional structure('bundles' to 'layers'), the second to a change from two-dimensional to three-dimensional structure ('layers' to 'clusters'), and the third at 2.40 is formation of the most rigid topology [27].

In this case, the authors have observed reversal in the trend at $\bar{Z} = 2.08$. XRD patterns shown in Fig. 1 clearly indicate that the addition of tin in Se–Te system changes the configuration by forming SnSe orthorhombic phases and $SnSe_2$ hexagonal phases. Since Sn is added at the cost of Se, therefore, one can expect that the probability of formation of $SnSe_2$ hexagonal phases decreases with the increase in Sn concentration. Beyond 4 at %, SnSe orthorhombic phases are formed in excess as compared with $SnSe_2$ hexagonal phases. Thus, the incorporation of Sn into Se chains for concentrations more than 4 at % of Sn is a process, which comparatively destroys less long Se-chains, thereby causing a change from one- to two-dimensional structure. This structural transformation is observed in the form of reversal in the increasing trend of dielectric constant and dielectric loss.

Tonchev and Kasap [29] also reported the reversal in the compositional dependences of T_g, C_p, ΔC_p, ΔH_g for the low concentration (0.01–1 at %) of Sb in glassy $Se_{100-x}Sb_x$ system. Saraswat and Kushwaha [30] were found the similar results in calorimetric study of specific heat Cp in glassy $Se_{100-x}Sb_x$ system. They observed that the variation of Cp reveals local extrema in the glassy $Se_{100-x}Sb_x$ system at $x = 4$ and $x = 8$. Thus, the present results support the observation of local extrema in different physical properties of chalcogenide glasses at lower coordination numbers.

Conclusions

The dielectric parameters of glassy $Se_{80-x}Te_{20}Sn_x$ ($x = 0$, 2, 4, 6) alloys are temperature and frequency dependent. Dielectric dispersion is found to occur in these alloys. The results of the dielectric constant and dielectric loss measurements show that Guintini's theory of dielectric dispersion of two electrons hopping over a potential barrier is applicable in the present case.

The composition dependence of dielectric constant, dielectric loss and activation energy of thermally activated ac conduction in the present glassy system show a reversal in the trend at $x = 4$. The appearance of these local extrema is explained in terms of changes from one- to two-dimensional structure.

References

1. Nishi J, Morimoto S, Inagawa I, Iizuka R, Yamashita T, Yamagishi T (1992) J Non-Cryst Solids 140:199
2. Seddon AB, Laine MJ (1997) J Non-Cryst Solids 168:213–214
3. Ohta T (2001) J Optoelectron Adv Mater 3:609
4. Zhou Gou-Fu (2001) Mater Sci Eng A 73:304
5. Lankhorst MHR (2002) J Non-Cryst Solids 297:210
6. Kolobov AV, Tominaga J (2002) J Optoelectron Adv Mater 4:679
7. Bureau B, Zhang XH, Smektala F, Adam J, Troles J, Ma H, Boussard-Pledel C, Lucas J, Lucas P, Coq DL, Riley MR, Simmons JH, Non-Cryst J (2004) Solids 276:345
8. Popescu M (2005) J Optoelectron Adv Mater 7:2189
9. Lezal D, Zavadil J, Prochazka M (2005) J Optoelectron Adv Mater 7:2281
10. Mehta N (2006) J Sci Indus Re 65:777
11. Harbold JM, Hilday FO, Wise FW, Itkain BG (2002) IEEE Photon Tech Lett 14:822
12. Onozuka A, Oda O (1988) J Non-Cryst Solids 103:289
13. Georgieva I, Nesheva D, Dimitrov D, Kozhukharov V (1993) J Non-Cryst Solids 160:105
14. Kaur G, Komatsu T, Thangaraj R (2000) J Mater Sci 35:903
15. Kumar S, Laxmi GBVS, Husain M, Zulfequar M (2006) Eur Phys J Appl Phys 35:155
16. Sharma V, Thakur A, Sharma J, Kumar V, Gautam S, Tripathi SK (2007) J Non-Cryst Solids 353:1474
17. Saraswat VK, Kishore V, Sharma DK, Saxena NS, Sharma TP (2007) Chalcogenide Lett 4:61
18. Gautam S, Shukla DK, Jain S, Goyal N (1998) Pramana 50:25
19. Guintini JC, Zanchetta JV, Jullen D, Eholle R, Hoenou P (1981) J Non-Cryst Solids 45:57
20. Elliott SR (1977) Phil Mag 36:1291
21. Stearn AE, Eyring H (1937) J Chem Phys 5:113
22. Glasstone S, Laidler KJ, Eyring H (1941) Theory of Rate processes. McGraw Hill, New York
23. Pollak P, Pike GE (1972) Phys Rev Lett 25:1449
24. Choudhary N, Kumar A (2004) Ind J Eng Mat Sci 11:55

25. Tanaka K (1989) Phys Rev B 39:1270
26. Thorpe MF (1983) J Non-Cryst Sol 57:355
27. Phillips JC (1979) J Non-Cryst Sol 34:153
28. Phillips JC (1981) J Non-Cryst Sol 43:37
29. Tonchev D, Kasap SO (1999) J Non-Cryst Sol 248:28
30. Saraswat S, Kushwaha SSS (2009) Philo Mag 89:322